



# Photon-counting detector computed tomography in thoracic oncology: revolutionizing tumor imaging through precision and detail

 Masahiro Yanagawa<sup>1</sup>  
 Midori Ueno<sup>1</sup>  
 Rintaro Ito<sup>2</sup>  
 Daiju Ueda<sup>3</sup>  
 Tsukasa Saida<sup>4</sup>  
 Ryo Kurokawa<sup>5</sup>  
 Koji Takumi<sup>6</sup>  
 Kentaro Nishioka<sup>7</sup>  
 Shunsuke Sugawara<sup>8</sup>  
 Satoru Ide<sup>9</sup>  
 Maya Honda<sup>10</sup>  
 Mami Iima<sup>11</sup>  
 Mariko Kawamura<sup>12</sup>  
 Akihiko Sakata<sup>13</sup>  
 Keitaro Sofue<sup>14</sup>  
 Seitaro Oda<sup>15</sup>  
 Tadashi Watabe<sup>1</sup>  
 Kenji Hirata<sup>16</sup>  
 Shinji Naganawa<sup>12</sup>

<sup>1</sup>The University of Osaka Graduate School of Medicine, Department of Diagnostic and Interventional Radiology, Osaka, Japan

<sup>2</sup>Nagoya University Graduate School of Medicine, Department of Innovative BioMedical Visualization, Nagoya, Japan

<sup>3</sup>Osaka Metropolitan University Graduate School of Medicine, Department of Artificial Intelligence, Osaka, Japan

<sup>4</sup>University of Tsukuba Institute of Medicine, Department of Radiology, Tsukuba, Japan

<sup>5</sup>The University of Tokyo Graduate School of Medicine, Department of Radiology, Tokyo, Japan

<sup>6</sup>Kagoshima University Graduate School of Medical and Dental Sciences, Department of Radiology, Kagoshima, Japan

<sup>7</sup>Hokkaido University Faculty of Medicine, Global Center for Biomedical Science and Engineering, Division of Radiation Oncology, Sapporo, Japan

<sup>8</sup>National Cancer Center Hospital, Department of Diagnostic Radiology, Tokyo, Japan

<sup>9</sup>University of Occupational and Environmental Health, Department of Radiology, Kitakyushu, Japan

<sup>10</sup>Kyoto University Hospital, Preemptive Medicine and Lifestyle-Related Disease Research Center, Kyoto, Japan

<sup>11</sup>Nagoya University Graduate School of Medicine, Department of Fundamental Development for Advanced Low Invasive Diagnostic Imaging, Nagoya, Japan

<sup>12</sup>Nagoya University Graduate School of Medicine, Department of Radiology, Nagoya, Japan

<sup>13</sup>Kyoto University Graduate School of Medicine, Department of Diagnostic Imaging and Nuclear Medicine, Kyoto, Japan

<sup>14</sup>Kobe University Graduate School of Medicine, Department of Radiology, Kobe, Japan

<sup>15</sup>Kumamoto University Faculty of Life Sciences, Department of Diagnostic Radiology, Kumamoto, Japan

<sup>16</sup>Hokkaido University Graduate School of Medicine, Department of Diagnostic Imaging, Sapporo, Japan

## ABSTRACT

Photon-counting detector computed tomography (PCD-CT) is an emerging imaging technology that promises to overcome the limitations of conventional energy-integrating detector (EID)-CT, particularly in thoracic oncology. This narrative review summarizes technical advances and clinical applications of PCD-CT in the thorax with emphasis on spatial resolution, dose-image-quality balance, and intrinsic spectral imaging, and it outlines practical implications relevant to thoracic oncology. A literature review of PubMed through May 31, 2025, was conducted using combinations of "photon counting," "computed tomography," "thoracic oncology," and "artificial intelligence." We screened the retrieved records and included studies with direct relevance to lung and mediastinal tumors, image quality, radiation dose, spectral/iodine imaging, or artificial intelligence-based reconstruction; case reports, editorials, and animal-only or purely methodological reports were excluded. PCD-CT demonstrated superior spatial resolution compared with EID-CT, enabling clearer visualization of fine pulmonary structures, such as bronchioles and subsolid nodules; slice thicknesses of approximately 0.4 mm and *ex vivo* resolvable structures approaching 0.11 mm have been reported. Across intraindividual clinical comparisons, radiation-dose reductions of 16%–43% have been achieved while maintaining or improving diagnostic image quality. Intrinsic spectral imaging enables accurate iodine mapping and low-keV virtual monoenergetic images and has shown quantitative advantages versus dual-energy CT in phantoms and early clinical work. Artificial intelligence-based deep-learning reconstruction and super-resolution can complement detector capabilities to reduce noise and stabilize fine-structure depiction without increasing dose. Potential reductions in contrast volume are biologically plausible given improved low-keV contrast-to-noise ratio, although clinical dose-finding data remain limited, and routine K-edge imaging has not yet translated to clinical thoracic practice. In conclusion, PCD-CT provides higher spatial and spectral fidelity at lower or comparable doses, supporting earlier and more precise tumor detection and characterization; future work should prioritize outcome-oriented trials, protocol harmonization, and implementation studies aligned with "Green Radiology".

## KEYWORDS

Artificial intelligence, cancer, computed tomography, diagnosis, iodine, radiation dose reduction, spatial resolution, spectral imaging

Handling editor: Furkan Ufuk

Corresponding author: Masahiro Yanagawa

E-mail: m-yanagawa@radiol.med.osaka-u.ac.jp

Received 17 July 2025; revision requested 11 August 2025; accepted 11 September 2025.



Epub: 24.09.2025

Publication date: 01.07.2026

DOI: 10.4274/dir.2025.253550

Computed tomography (CT) plays a pivotal role in thoracic imaging, offering invaluable insights for the diagnosis, staging, and monitoring of various pulmonary conditions, particularly in oncology. However, conventional energy-integrating detector (EID)-CT systems have limitations, including restricted spatial resolution, higher image noise, and an inability to differentiate materials based on their spectral properties. These limitations can hinder the precise characterization of subtle pathological abnormalities, such as early-stage lung nodules and complex interstitial lung diseases. Photon-counting detector CT (PCD-CT) has emerged as a revolutionary imaging modality that addresses many of these challenges, promising to alter clinical practice in thoracic oncology fundamentally. Conventional EID-CT converts X-rays into scintillation light, requiring separators that limit spatial resolution and efficiency; furthermore, light-to-current conversion introduces electronic noise, reducing image quality and accuracy. In contrast, PCD-CT converts photons directly into electrical signals without noise, offering theoretically superior spatial resolution (0.11 mm in-plane, 0.20 mm along the body axis) and multi-energy information for precise X-ray energy analysis (Figure 1). As a result of these structural differences, PCD-CT offers a range of advantages, including significantly improved spatial resolution, reduced image noise, and multi-energy spectral imaging capabilities.<sup>1-10</sup> These advancements result in clearer, more detailed images, even at reduced radiation exposure levels. The clinical utility of PCD-CT in chest imaging is rapidly expanding, with reports demonstrating its

efficacy in improving visualization of bronchi and vessels,<sup>7,9,11</sup> enhancing the detection of emphysema and post-coronavirus disease-2019 lung abnormalities,<sup>6,10,12,13</sup> increasing diagnostic confidence in interstitial pneumonia-related findings, such as reticulation,<sup>6,10,14,15</sup> and improving image quality for pulmonary embolism assessment.<sup>10,16</sup> Beyond these immediate clinical benefits, PCD-CT's inherent capabilities for a sizeable radiation dose reduction and potential for lower contrast agent usage align with the growing concept of Green Radiology. This paradigm emphasizes environmentally sustainable and patient-safe radiological practices, making PCD-CT a key technology for minimizing the ecological footprint and patient burden of medical imaging. Lung cancer, with its diverse histological types and heterogeneous nature, presents a major diagnostic challenge. Accurate preoperative assessment of lung tumors, including the grading of lung adenocarcinoma and the estimation of invasive components, is crucial for guiding treatment strategies and predicting patient prognosis.<sup>17-19</sup> Although conventional CT has offered valuable insights, its ability to evaluate these subtle tumor characteristics precisely has been limited. Furthermore, the integration of cutting-edge artificial intelligence (AI) with PCD-CT is poised to revolutionize tumor imaging further. Deep learning reconstruction (DLR) algorithms, for instance, can markedly reduce image noise while preserving spatial resolution, surpassing the capabilities of traditional iterative reconstruction algorithms.<sup>11,20</sup> This synergistic collaboration between advanced detector technology and AI holds immense potential to enhance image quality and diagnostic confidence in lung tumor evaluation, paving the way for more precise and personalized oncology care.

Although PCD-CT holds promise across a wide range of anatomical regions, this review particularly emphasizes its application in thoracic oncology imaging due to its clinical importance. The aim is to outline comprehensively the transformative impact of PCD-CT in this field, highlighting advancements in spatial resolution, the critical balance between image quality and radiation dose reduction, and the novel insights enabled by its spectral imaging capabilities. By exploring these key areas, we highlight how PCD-CT is revolutionizing tumor imaging through unprecedented precision and detail, ultimately leading to improved diagnostic performance and patient outcomes.

## Methods of literature review

This work is a narrative review focusing on PCD-CT in thoracic oncology, synthesizing technical advances in spatial resolution, the balance between dose and image quality, and spectral/iodine imaging, and considering their clinical implications for lung and mediastinal tumors. The PubMed database was searched through May 31, 2025, using combinations of "photon counting," "photon-counting detector," "computed tomography," "thoracic," "lung," "mediastinum," "oncology," and "artificial intelligence." After deduplication, titles and abstracts were screened, and full texts were assessed. The priorities were as follows: comparisons of intra-individual PCD-CT versus EID-CT; thoracic oncology endpoints (nodule characterization, staging adjuncts, treatment response, surveillance/complications); trade-offs between dose and image quality; spectral/iodine quantification; and AI/DLR analyses. In total, 323 records were screened, and 68 studies were included in the qualitative synthesis; to avoid implying a systematic review, a flow diagram is not provided, and a meta-analysis was not performed. Animal-only studies, purely methodological papers without thoracic relevance, editorials/case reports/letters, and duplicate analyses without additional information were excluded.

## Comparison of spatial resolution between energy-integrating detector and photon-counting detector computed tomography

Building upon the foundational advancements outlined in the introduction, one of the most compelling advantages of PCD-CT in thoracic imaging is its inherently superior spatial resolution compared with traditional EID-CT (Figure 2). This enhanced capability stems directly from the ability of PCD-CT to count individual photons and precisely categorize them by energy. This fundamental difference in detection methodology minimizes signal loss and electronic noise, thereby allowing for the acquisition of data with finer detail and leading to a notable improvement in image sharpness and the ability to discern minute anatomical structures.<sup>1-12</sup> Clinical studies have provided robust evidence of superior spatial resolution on PCD-CT and its direct impact on diagnostic image quality. Inoue et al.<sup>12</sup> conducted a prospective clinical study in adult patients undergoing low-dose lung cancer screening, in which three readers directly compared PCD-CT and EID-CT using a 5-point Likert scale (−2 to +2).

### Main points

- Photon-counting detector computed tomography (PCD-CT) offers markedly improved spatial and spectral resolution compared with conventional energy-integrating detector CT, allowing for more accurate detection and characterization of thoracic tumors, including subsolid nodules and early-stage lung cancer.
- PCD-CT substantially reduces radiation doses by up to 40% without compromising image quality and shows promise in reducing contrast agent volume, contributing to safer and more sustainable imaging.
- The integration of artificial intelligence and spectral imaging techniques with PCD-CT enhances diagnostic precision and aligns with the principles of Green Radiology, supporting both clinical excellence and environmental responsibility.

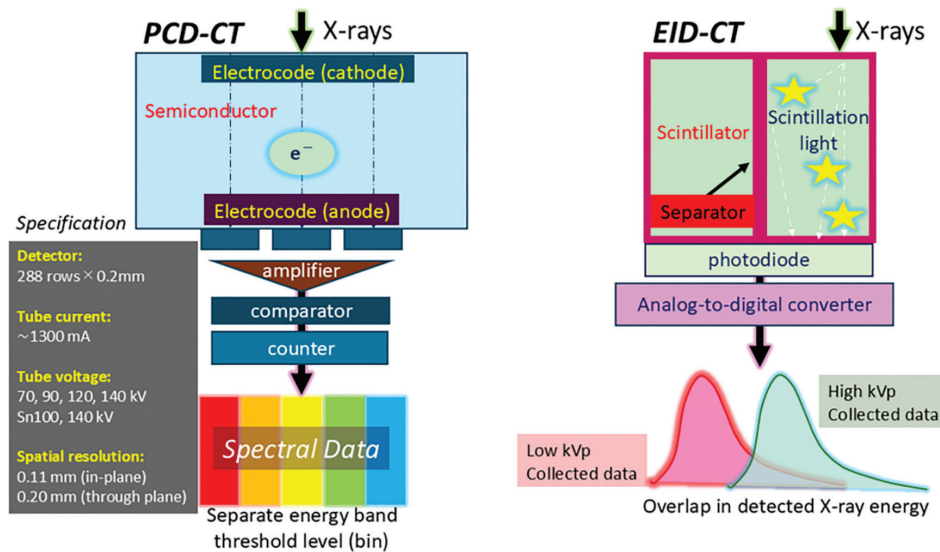


**Figure 1.** Comparison of signal conversion processes in energy-integrating detector computed tomography (EID-CT) and photon-counting detector (PCD)-CT. Conventional scintillator-type detector (EID)-CT devices convert incident X-rays into scintillation light containing all spectral information for processing, and separators are required to prevent light from diffusing to adjacent detection elements. The thickness of the separator limits spatial resolution and reduces X-ray usage efficiency, and the electrical noise generated when converting light into electric current degrades image quality and quantitative performance. In comparison, PCD-CT collects X-rays by energy and converts electrons directly into an electric current; therefore, there is no electrical noise. Theoretically, it provides higher spatial resolution than conventional CT (0.11 mm in plane, 0.20 mm in body axis direction) and multi-energy information for each X-ray energy, enabling highly accurate X-ray energy analysis.

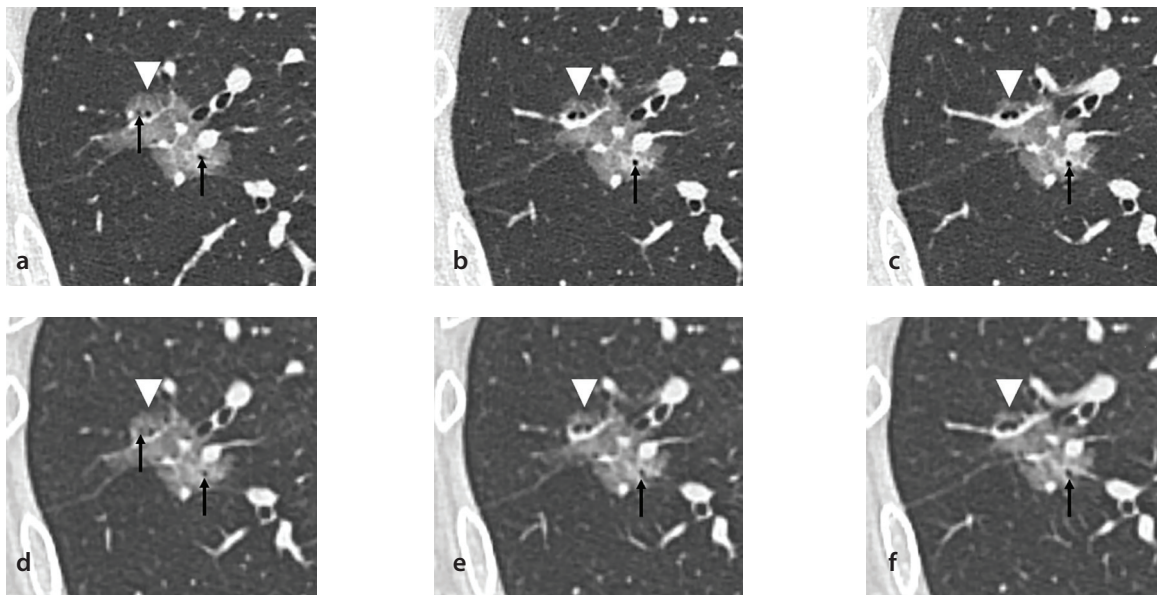


**Figure 2.** Comparison of photon-counting computed tomography (CT) images (a-c) and energy-integrating detector (EID)-CT images (d-f) in a 72-year-old woman with lung adenocarcinoma. The photon-counting CT images [CT dose index volume (CTDIvol), 9.2 mGy; matrix size, 512; and slice thickness, 0.4 mm] demonstrate clearer depiction of air bronchogram (black arrows) within the nodule and the nodule margins (white arrow heads) than the EID-CT images (CTDIvol, 12.8 mGy; matrix size, 512; and slice thickness, 0.625 mm).

Their findings revealed that PCD-CT provided significantly superior delineation of lung nodule boundaries ( $+0.8 \pm 0.9$ ,  $P < 0.001$ ) and improved visualization of emphysema ( $+0.3 \pm 0.6$ ,  $P < 0.001$ ). PCD-CT was consistently rated superior for image sharpness (mean score  $+0.8$ ,  $P < 0.001$ ), despite the use of a similar reconstruction kernel. Two of the three readers also reported significantly higher overall diagnostic quality ( $+0.3$  to  $+0.7$ ,  $P < 0.001$ ).

Similarly, Wang et al.<sup>21</sup> demonstrated PCD-CT's advanced capability in characterizing subsolid nodules, noting its superiority over EID-CT in depicting subtle nodule features, with the exception of lobulation. This study also highlighted a crucial technical aspect, concluding that 0.4 mm slice thickness PCD-CT images achieved an optimal balance between ultra-high resolution and subjective diagnostic image quality, which is crucial for

guiding clinical imaging protocols. Furthermore, Bartlett et al.<sup>9</sup> investigated the impact of higher matrix reconstruction (e.g., 1,024 matrix) with PCD-CT, reporting improved visualization of higher-order bronchi and bronchial wall clarity, suggesting the clinical benefit of the enhanced technical resolution capabilities inherent to PCD-CT systems.

Further compelling evidence for the high spatial resolution of PCD-CT comes from *ex vivo* studies using human tissues, which bridge the gap between technical capabilities and direct clinical relevance. Hata et al.<sup>11</sup> performed a detailed comparative analysis of PCD-CT and EID-CT using inflated cadaveric human lungs. This unique study design allowed for the precise evaluation of the technologies on human tissue without the confounding effects of physiological motion. The study confirmed that PCD-CT depicted lung nodules and airway microstructure with significantly greater clarity than EID-CT. A pivotal finding was the quantification of PCD-CT's detection limit, demonstrating its capability to detect nodules and airways with a median diameter of approximately 600  $\mu\text{m}$ . The maximum spatial resolution achieved in this study was 0.11 mm, emphasizing its extraordinary ability to resolve microscopic anatomical details.<sup>11</sup> These findings underscore the current ability of PCD-CT to provide unprecedented information on subtle pulmonary structures. In a clinical context,<sup>6,20</sup> this means a higher potential for earlier detection and more precise characterization of a wide range of lung diseases, including incipient lung cancers, thereby facilitating earlier intervention and improved patient outcomes. In the future, this enhanced spatial resolution is expected to become a cornerstone for refined disease staging, personalized treatment planning, and potentially even the identification of novel imaging biomarkers for prognosis and treatment response in thoracic oncology. See "Thoracic Oncology Tasks and PCD-CT Advantages: Evidence Map" in Table 1.

### Radiation dose reduction without degradation of spatial resolution in photon-counting detector computed tomography

Researchers have conducted many studies on conventional EID-CT and have investigated and implemented radiation dose reduction strategies, implying the importance of dose management.<sup>22-33</sup> Radiation dose is a critical consideration in all CT examinations, and minimizing patient exposure is a fundamental principle of radiological practice.

Recent clinical studies have provided compelling evidence that PCD-CT can achieve substantial radiation dose reductions compared with EID-CT.<sup>12,21,34,35</sup> These reductions are clinically meaningful, especially in the context of lung cancer screening programs and long-term oncologic surveillance, where cumulative dose becomes a significant concern. As noted in the previous section, Inoue et al.<sup>12</sup> revealed the utility of

PCD-CT in evaluating nodule boundaries and visualization of emphysema. Crucially, these improvements were achieved concurrently with a significantly lower average CT dose index volume, demonstrating an approximate 16.4% reduction (0.61 mGy vs. 0.73 mGy,  $P < 0.001$ ) compared with EID-CT. Similarly, Wang et al.<sup>21</sup> further corroborated PCD-CT's benefit in characterizing subsolid nodules. Their study demonstrated that PCD-CT not only improved lesion depiction but also delivered a significantly reduced effective dose, quantifying an approximate 17.5% reduction ( $1.79 \pm 0.39$  mSv vs.  $2.17 \pm 0.57$  mSv,  $P < 0.001$ ) compared with EID-CT. Overall, various clinical studies have demonstrated significant dose reductions with PCD-CT compared with EID-CT, generally ranging from approximately 16% to over 40% depending on the specific comparison and protocol. The dose-reduction benefit of PCD-CT extends to specific vulnerable patient populations and advanced imaging protocols where dose optimization is critical. Early studies with PCD-CT in pediatric chest imaging of cystic fibrosis have reported average effective doses as low as 0.12 mSv,<sup>36</sup> a remarkable reduction compared with even ultra-low-dose EID-CT protocols, which can be approximately 0.15 mSv for combined inspiratory and expiratory chest CT in pediatric populations.<sup>37</sup> For adults with cystic fibrosis, PCD-CT has demonstrated effective doses as low as 0.55 mSv, representing a 42% reduction compared with EID-CT protocols for similar diagnostic tasks.<sup>34</sup> PCD-CT has notably demonstrated a 31% lower effective dose to red bone marrow than EID-CT<sup>34</sup> in younger cohorts, where the risk of radiation-induced malignancy is a significant concern.<sup>38,39</sup> Although conventional low-dose EID-CT protocols for chest imaging typically report effective radiation doses ranging from 1.5 mSv to 2.0 mSv,<sup>40,41</sup> PCD-CT has shown substantial advancements; its substantial dose reduction capabilities offer promising benefits for enhancing patient safety in routine clinical practice.<sup>42</sup> Furthermore, the advantages of PCD-CT also extend to comparisons with other advanced CT modalities, such as dual-energy CT (DECT). Hagen et al.<sup>43</sup> performed a clinical comparison of contrast-enhanced chest imaging, a cornerstone for evaluating tumor vascularity and treatment response, using PCD-CT versus a second-generation dual-source DECT in oncology patients. They reported that PCD-CT provided significantly higher tumor-to-lung parenchyma contrast ratios, indicating enhanced tumor conspicuity and delineation. Importantly, PCD-CT maintained equivalent or superior image quality while achieving a substantial 43%

reduction in radiation dose compared with a second-generation dual-source DECT.<sup>43</sup> This robust clinical evidence directly confirms PCD-CT's impressive dose efficiency and image quality benefits in a demanding patient cohort undergoing oncologic imaging.

PCD-CT has the potential to reduce contrast agent usage in thoracic oncology diagnosis. Sawall et al.<sup>44</sup> compared PCD-CT with EID-CT using phantoms containing various iodine concentrations (ICs) and demonstrated improvements in the contrast-to-noise ratio (CNR) of up to 30% with a single energy bin and up to 37% with optimal two-bin weighting, corresponding to a potential reduction in contrast medium dose of up to 37%.<sup>44</sup> In addition, several studies have reported that PCD-CT enables a 25%–50% reduction in contrast medium dose in head and neck CT angiography (CTA) or coronary CTA while maintaining diagnostic image quality or CNR.<sup>45,46</sup> Such a contrast medium dose reduction may be particularly beneficial for patients with impaired renal function and elderly populations.

These clinical investigations collectively demonstrate that PCD-CT offers a compelling combination of maintained or improved image quality and significant dose reduction across various clinical scenarios pertinent to thoracic oncology. This improved benefit-risk ratio represents a major advancement in CT, positioning PCD-CT as an invaluable tool, particularly for lung cancer screening programs and long-term oncologic follow-up, where repeated examinations are common. Crucially, this unique synergy of imaging quality, dose efficiency, and potential for contrast medium dose reduction also strongly aligns with the burgeoning principles of Green Radiology, emphasizing the minimization of patient exposure and the promotion of environmentally sustainable imaging practices. This comprehensive advantage solidifies PCD-CT's role as a cornerstone for optimizing patient care and advancing diagnostic capabilities in thoracic imaging.

### Artificial intelligence technology for super-resolution

This AI-based super-resolution subsection may be useful to clarify achievable EID-CT resolution, complement PCD-CT in practice, and support detector-aware harmonization across EID-CT and PCD-CT data.

The field of medical imaging continues to advance rapidly, driven by innovations in detector hardware and post-processing algorithms.<sup>20,28,47-51</sup>

**Table 1.** Thoracic oncology tasks and photon-counting detector computed tomography (PCD-CT) advantages: evidence map

Clinical task	Specific question	Typical comparator	Study type (examples)	Primary metrics (examples)	Reported signal	Clinical implication	References
<b>Lung cancer screening</b> (low-dose nodule detection)	Does PCD-CT improve detection and clarity of small pulmonary nodules at low radiation doses, compared with standard low-dose computed tomography (CT)?	Conventional low-dose energy-integrating detector CT (EID-CT)	Prospective intra-individual comparisons; feasibility trials in screening populations	Nodule detection rate; small nodule boundary visibility; image noise; CT dose index volume (radiation dose)	↑ (Improved)	Earlier detection of lung cancer with sharper nodule depiction at reduced dose, enhancing screening efficacy while lowering radiation risk	8,12
<b>Subsolid nodule characterization</b> (invasive vs. indolent)	Can PCD-CT better characterize subsolid (ground-glass or part-solid) lung nodules and assess invasive components versus conventional CT?	Thin-section EID-CT (standard high-res)	Paired same-day patient studies (PCD-CT vs. EID-CT in each patient)	Lesion conspicuity and demarcation; CT attenuation of solid component; radiologist invasiveness classification; effective dose	↑ (Improved)	More accurate non-invasive assessment of tumor invasiveness, aiding surgical decision-making (e.g., suitability for sublobar resection) while also reducing patient dose	21,58
<b>Tumor morphology and margins</b> (solid tumor evaluation)	Does PCD-CT provide clearer visualization of tumor margins and fine morphological features (e.g., spiculation, lobulation) compared with conventional CT?	High-resolution EID-CT (ultra-thin slices with iterative recon)	<i>Ex vivo</i> cadaver lung comparisons; prospective clinical studies with artificial intelligence super-resolution reconstruction	Spatial resolution (achieved voxel size); minimum detectable lesion size; clarity of edge features (spiculation, air bronchograms); reader confidence scores	↑ (Improved)	Enhanced delineation of tumor extent and characteristics, improving lesion characterization and aiding precise surgical or radiotherapy planning	9,20
<b>Lymph node staging</b> (mediastinal metastasis detection)	Can PCD-CT spectral imaging improve identification of metastatic lymph nodes in thoracic malignancies compared with standard CT or dual-energy CT?	Contrast-enhanced EID-CT or dual-energy CT (with iodine mapping)	Retrospective clinical spectral CT studies (with surgical pathology as reference); phantom iodine-detection experiments	Iodine concentration in nodes (correlation with malignancy); virtual monoenergetic imaging clarity; minimum detectable iodine level (phantom)	↑ (Improved)	Potential for more accurate non-invasive nodal staging – improved detection of nodal metastases due to superior contrast and spectral sensitivity, possibly reducing need for invasive sampling	63,64
<b>Treatment response assessment</b> (therapy monitoring)	Does PCD-CT improve the evaluation of tumor response to therapy (e.g., changes in size or enhancement) compared with conventional CT?	Standard contrast-enhanced CT (EID-CT or latest dual-source CT)	Preliminary clinical comparisons in oncology patients (PCD-CT vs. dual-source CT)	Tumor-to-lung contrast ratio; lesion conspicuity on follow-up; image noise and SNR; dose per scan	↑ (Improved)	Clearer visualization of residual tumor and subtle changes in enhancement or size, facilitating more confident assessment of treatment efficacy while minimizing radiation and contrast burden	43

SNR, signal-to-noise ratio.

Among the most promising developments is the application of AI, particularly super-resolution techniques based on deep learning, to improve the spatial resolution of CT imaging beyond the physical limits of existing systems.<sup>52,53</sup> These methods can reconstruct high-resolution images from lower-resolution data, effectively enhancing fine structural details essential for accurate diagnosis and treatment planning (Figure 3).

Although advances in CT spatial resolution have often focused on detector innovations, particularly photon-counting systems, conventional EID-CT has also demonstrated substantial diagnostic capabilities by employing high-matrix imaging. For instance, Yanagawa et al.<sup>54</sup> used a  $2,048 \times 2,048$  matrix with a 0.25 mm slice thickness on an EID-CT to evaluate invasive lung adenocarcinomas. Their findings showed excellent diagnostic performance for identifying features such as disrupted air bronchograms and solid components  $>0.8$  cm, with a sensitivity of 97% and specificity of 86% [area under the curve (AUC), 0.94]. These results suggest that enhancing spatial resolution could lead to more accurate lung cancer evaluations. In

addition, high-resolution EID-CT imaging may influence computational approaches, such as radiomics. Ninomiya et al.<sup>55</sup> demonstrated that CT images reconstructed with a 1,024 matrix improved the radiomic prediction of solid and micropapillary components in invasive lung adenocarcinoma, highlighting the potential benefits of high-spatial-resolution input data in image-based feature analysis.

Parallel to these CT hardware-based improvements, AI-based super-resolution techniques have emerged as a promising approach to further enhance CT image quality. Kim et al.<sup>56</sup> demonstrated that applying a three-dimensional (3D) deep learning super-resolution algorithm to thick-slice CT data significantly reduced volumetric measurement error (from 52.2% to 15.7%) and improved Lung Imaging Reporting and Data System categorization accuracy (from 72.7% to 94.5%). Similarly, super-resolution radiomics has been shown to increase the predictive accuracy of histologic subtypes in lung cancer. In a cohort of 245 patients, Xing et al.<sup>57</sup> reported an AUC improvement from 0.761 to 0.819 for the detection of micropapillary

and solid components. A multicenter study also found that a super-resolution CT pipeline combined with an SE-ResNet50 model achieved superior prediction of spread through air spaces, with an AUC of 0.806 compared with 0.695 for standard models.<sup>58</sup>

Among these AI-based approaches, Precise IQ Engine (PIQE; Canon Medical Systems, Otawara, Japan) represents a clinically implemented, super-resolution DLR technique tailored for EID-CT systems. The PIQE system uses a 3D convolutional neural network trained on paired low- and high-resolution images derived from ultra-high-resolution CT, enabling the reconstruction of low-noise, high-resolution images without increased radiation dose. Notably, it supports high-matrix reconstruction (up to  $1,024 \times 1,024$ ), providing sharper spatial detail and preserving image texture.<sup>52,53</sup> Although most validation studies of PIQE have focused on coronary and abdominal CT, its technical design suggests considerable potential in thoracic oncology. Enhanced spatial resolution and reduced blooming artifacts may improve the delineation of lesion margins, internal heterogeneity, and subtle features, such as broncho-

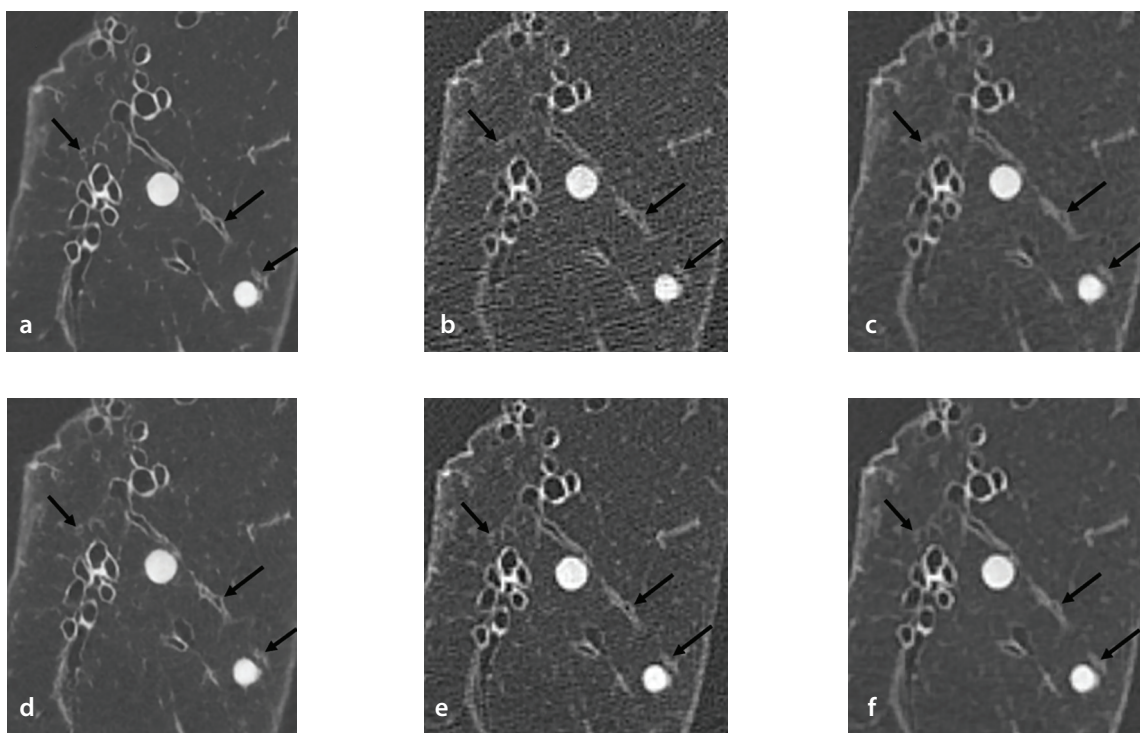


**Figure 3.** Comparison of images acquired at 8.5 mGy and 2.2 mGy, where the dose refers to the computed tomography dose index volume, using different reconstruction methods in a human cadaveric lung with lung metastases. Images include 8.5 mGy-FBP (matrix size, 512; slice thickness, 0.5 mm; (a)), 8.5 mGy-AiCE (matrix size, 512; slice thickness, 0.5 mm; (b)), 8.5 mGy-PIQE (matrix size, 1024; slice thickness, 0.5 mm; (c)), 2.2 mGy-FBP (matrix size, 512; slice thickness, 0.5 mm; (d)), 2.2 mGy-AiCE (matrix size, 512; slice thickness, 0.5 mm; (e)), and 2.2 mGy-PIQE [matrix size, 1024; slice thickness, 0.5 mm; (f)]. 8.5 mGy-AiCE (b) reduces image noise compared with 8.5 mGy-FBP (a). 8.5 mGy-PIQE (c) further enhances the visualization of bronchiolar walls (black arrows) due to the higher matrix size and higher noise reduction. At a lower dose, 2.2 mGy-FBP (d) shows increased noise, whereas 2.2 mGy-AiCE (e) mitigates it. Notably, 2.2 mGy-PIQE (f) preserves superior delineation of bronchiolar structures despite the reduced dose. FBP, filtered back projection; AiCE, advanced intelligent Clear-IQ Engine, which is a deep learning reconstruction (DLR) technique; PIQE, precise IQ Engine, which is a super-resolution DLR technique.

vascular invasion. These improvements are particularly relevant for image-based staging and treatment planning in lung cancer. Moreover, the use of high-fidelity input data is increasingly recognized as critical in radiomics and AI-based prediction models. Thus, PIQE-enabled super-resolution CT may not only enhance visual interpretation but also improve the performance of computational tools in thoracic oncology.

Although PCD-CT inherently offers enhanced spatial resolution through its advanced detector design, recent studies have highlighted the added value of integrating AI-based reconstruction algorithms. Sasaki et al.<sup>20</sup> investigated a cadmium zinc telluride-based PCD-CT system combined with DLR and demonstrated that ultra-high-resolution images provided clearer delineation of key morphological features, such as spiculation and lobulation. These features are particularly important for the characterization of lung cancer. The observed improvements contributed to greater diagnostic confidence and suggest that AI-based super-resolution techniques can further enhance the clinical utility of PCD-CT in thoracic oncology. Together, these developments demonstrate that AI-enabled super-resolution contributes not only to improved image aesthetics but also to enhanced diagnostic precision and prognostic assessment. Whether applied to EID-CT or PCD-CT, and whether implement-

ed through high-matrix acquisition or DLR, these techniques enable better visualization of subtle but clinically significant features, support more robust radiomic analyses, and allow for earlier and more accurate diagnosis of thoracic malignancies. As AI-driven reconstruction becomes increasingly integrated into clinical workflows, further validation across diverse patient populations and imaging settings will be essential. Nonetheless, the convergence of advanced detector technologies, high-resolution matrix design, and deep learning-based image enhancement represents a promising foundation for the next generation of precision imaging in thoracic oncology.

### Spectral imaging with photon-counting detector computed tomography: technical advances and clinical implications in comparison with dual-energy computed tomography

Spectral imaging has emerged as a pivotal advancement in CT, enabling compositional and quantitative assessments that surpass the capabilities of conventional, attenuation-based imaging. DECT, which achieves spectral differentiation through dual-source acquisition, rapid kilovoltage switching, or layered detectors, has long been used in clinical settings. In thoracic oncology, DECT has proven particularly useful in iodine quantification, which aids in tumor characteriza-

tion and assessment of treatment response. However, DECT is limited by binary energy separation, spectral overlap, and reduced material specificity.<sup>59-63</sup> PCD-CT represents a transformative advancement in spectral imaging. Unlike EID-CT, PCD-CT systems utilize semiconductor materials, such as cadmium zinc telluride, to directly count individual X-ray photons and classify them by energy.<sup>1-10</sup> This novel detector architecture enables simultaneous multi-energy acquisition with superior energy resolution and reduced electronic noise. Furthermore, PCD-CT inherently provides higher spatial resolution due to smaller detector elements and reduced cross-talk. These features collectively contribute to more accurate material decomposition, enhanced signal-to-noise ratio (SNR), and the potential for lower radiation doses. These advantages are expected to enhance diagnostic performance across a broad range of clinical applications, including thoracic oncology. A comparison of the spectral imaging capabilities of DECT and PCD-CT is summarized in Table 2, illustrating the technical distinctions and clinical implications relevant to thoracic tumor evaluation. As the table indicates, PCD-CT surpasses DECT in energy resolution, spatial resolution, signal-to-noise characteristics, and spectral quantification accuracy, representing a next-generation platform for spectral thoracic oncology imaging (Figures 4, 5).

**Table 2.** Technical comparison between dual-energy computed tomography (DECT) and photon-counting detector computed tomography (PCD-CT) for spectral thoracic imaging

Feature	DECT	PCD-CT
Detector type	Energy-integrating detector (EID)	Photon-counting semiconductor detector (e.g., cadmium zinc telluride)
Energy resolution	Binary (low)	Multi-bin (high)
Spectral acquisition	Two spectra via dual-source/kVp switching, dual-layer/split filter	Simultaneous multi-energy per photon
Virtual monochromatic imaging quality	Available (noisy at low keV)	Available (low-noise, high fidelity)
Material decomposition	Limited to two-material basis	Multi-material decomposition feasible
K-edge imaging	Not supported	Supported (e.g., iodine, gadolinium, gold)
Spatial resolution	Limited by detector and noise	Higher due to small pixel and low noise
Signal-to-noise ratio	Moderate	High
Quantitative accuracy	Limited by beam hardening, overlap	Superior accuracy, artifact-resistant
Contrast efficiency	Requires higher dose	Enhanced at lower dose
Dose efficiency	Variable, protocol-dependent	Low-dose with high image quality
Tumor evaluation	Effective for iodine concentration (IC), Zeff, and extracellular volume fraction in mediastinal tumors	Superior delineation, quantification, and functional imaging
Nodal evaluation	Correlation between IC and nodal metastasis shown	Potential for improved nodal characterization with higher resolution
Artificial intelligence integration	Available	Available and ongoing

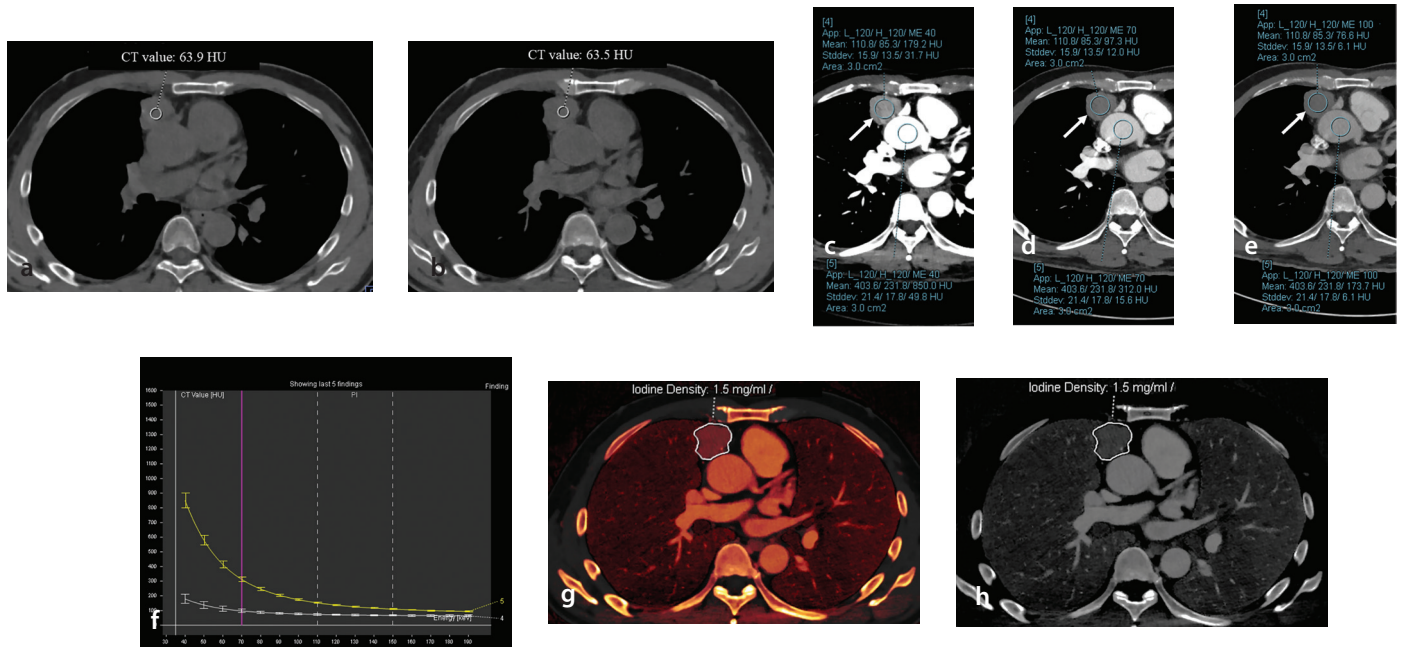


**Figure 4.** Spectral images from photon-counting computed tomography (CT) in a 51-year-old man with thymoma. On the true non-contrast image (a) in the mediastinal window, the CT value within the region of interest (circle) is 63.9 Hounsfield units (HU). On the virtual non-contrast image (b) reconstructed from the 120-second delayed scan, the CT value within the region of interest (circle) is 63.5 HU, which is nearly identical to that of the true non-contrast image. Monochromatic images reconstructed of 40 keV (c), 70 keV (d), 100 keV (e) from the 120-second delayed scan, and spectral HU curve (f) are shown. At 40 keV (c), the contrast of the anterior mediastinal mass (white arrows) and blood vessels is enhanced compared with 70 keV (d) and 100 keV (e). The spectral HU curve (f) indicates a change of CT values at each keV level in the tumor (white line) and the aorta (yellow line). The pink line indicates the 70 keV energy level. Iodine maps at a 120-second delay (g, color map; h, gray scale map) show an iodine concentration of 1.5 mg/mL in the region of interest.

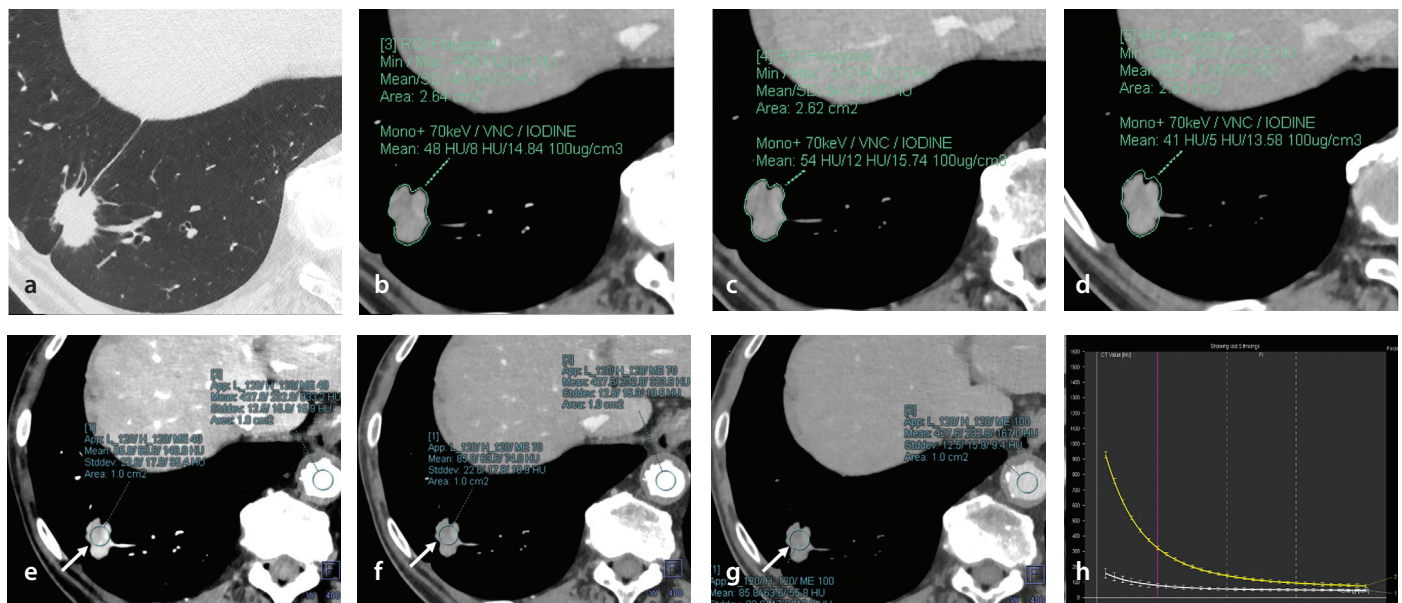


**Figure 5.** Photon-counting detector computed tomography (CT) images in an 80-year-old man with lung adenocarcinoma. (a) Shows the lung window CT images (matrix size, 512; and slice thickness, 0.4 mm). (b-d) Shows the mediastinal window CT images obtained at 60 seconds (b), 120 seconds (c), and 180 seconds (d) after contrast administration. At 60 seconds (b), the mean CT value of the nodule is 48 Hounsfield units (HU), and the iodine concentration (IC) is 1.484 mg/cm<sup>3</sup> (originally expressed in units of 100 µg/cm<sup>3</sup>). At 120 seconds (c), the mean CT value is 54 HU, with an IC of 1.574 mg/cm<sup>3</sup>. At 180 seconds (d), the mean CT value is 41 HU, and the IC is 1.358 mg/cm<sup>3</sup>. Monochromatic images reconstructed of 40 keV (e), 70 keV (f), 100 keV (g) from the 60-second delayed scan, and spectral HU curve (h) are shown. At 40 keV (e), the contrast of the lung nodule (white arrows) and blood vessels is enhanced compared with 70 keV (f) and 100 keV (g). The spectral HU curve (h) indicates a change of CT values at each keV level in the nodule (white line) and the aorta (yellow line). The pink line indicates the 70 keV energy level.

DECT has emerged as a valuable tool in thoracic oncology, with iodine-based quantification playing a key role in its diagnostic utility. For example, Deng et al.<sup>61</sup> demonstrated that DECT-derived spectral parameters, including IC, effective atomic number, and spectral slope, enabled differentiation between invasive thymic epithelial tumors and mediastinal lung cancers with high diagnostic accuracy (AUC: 0.88). Similarly, Takumi et al.<sup>62</sup> reported that IC and extracellular volume fraction, measured during the equilibrium phase using dual-layer DECT, were significantly elevated in thymic carcinoma. These findings support their usefulness in tumor subtyping. Additionally, DECT-based iodine mapping has been utilized for nodal staging. Huang et al.<sup>63</sup> showed that IC measurements correlated well with histopathologic nodal status in patients with lung adenocarcinoma, suggesting a role for spectral imaging in non-invasive lymph node evaluation. Building upon these advances, PCD-CT offers further improvements through its inherently higher spectral and spatial resolution. In a phantom study of mediastinal lesions, Centen et al.<sup>64</sup> demonstrated that PCD-CT could detect ICs as low as 0.238 mg/mL in 5 mm lesions when using low-keV virtual monoenergetic imaging and a high-resolution matrix. This performance significantly surpassed that of conventional CT, even when the radiation dose was reduced by 66%. These dose-saving and contrast-optimization capabilities not only improve diagnostic safety but also align with the principles of Green Radiology, which emphasize environmentally sustainable and patient-centered imaging practices. Furthermore, Vrbaski et al.<sup>65</sup> showed that PCD-CT achieved more accurate iodine quantification than DECT under low-dose conditions. The bias observed with PCD-CT was substantially lower, indicating a higher level of quantitative precision. Collectively, these studies highlight the growing importance of spectral CT imaging in thoracic oncology and suggest that PCD-CT is a promising next-generation imaging modality. With its excellent energy discrimination, improved image fidelity, and dose efficiency, PCD-CT will be a powerful tool for tumor characterization, lymph node evaluation, and personalized treatment planning in future clinical settings.

In addition to quantitative improvements, PCD-CT offers high spectral resolution by capturing individual photon energies, enabling advanced imaging techniques such as K-edge imaging. This method takes advantage of the sudden increase in photoelectric

absorption at the K-edge of specific high-Z elements (e.g., gold, gadolinium, iodine), allowing their selective detection and quantification. In a foundational phantom study, Si-Mohamed et al.<sup>66</sup> demonstrated the feasibility of multi-material decomposition using spectral PCD-CT. They achieved accurate quantification and discrimination of mixed contrast agents—including iodine, gadolinium, and gold nanoparticles—with high linearity (Pearson correlation coefficient  $\geq 0.97$ ) and low cross-contamination (root mean square error  $\leq 0.47$  mg/mL). This “multi-color” imaging was unattainable with conventional CT or DECT, highlighting the advantage of PCD-CT for detecting multiple agents within a single scan.<sup>66</sup> However, a practical limitation of K-edge imaging with PCD-CT is that clinically approved doses of contrast agents, such as gadolinium, may not produce a sufficient SNR for accurate material decomposition.<sup>67</sup> Phantom studies have generally required higher-than-clinical concentrations to achieve reliable K-edge detection. This raises concerns about the feasibility of directly applying these protocols in clinical practice. Although K-edge imaging with PCD-CT has shown clear feasibility and high quantitative accuracy in phantom and preclinical studies, clinical translation remains limited. This is mainly due to the lack of contrast agents specifically approved for K-edge imaging and the current need for elevated doses to ensure adequate image quality. At present, no clinical studies have reported the use of K-edge imaging in human patients.

### Summary and future directions

PCD-CT is redefining thoracic oncologic imaging by delivering unmatched spatial and spectral resolution, improved diagnostic confidence, and substantial reductions in radiation dose. Its ability to detect individual X-ray photons and measure their energy enables more accurate tumor characterization, earlier detection of small lesions, and advanced spectral imaging. These strengths are further enhanced by AI-based reconstruction techniques that improve image quality while maintaining diagnostic precision. PCD-CT is expected to play a central role in the future of precision imaging. Techniques such as K-edge imaging and multi-material decomposition may offer new insights into tumor biology, although further work is needed to adapt K-edge contrast agents for routine clinical use. Moreover, PCD-CT is well aligned with the concept of Green Radiology, which promotes safe, sustainable, and patient-centered imaging practices. As

Rockall et al.<sup>68</sup> have noted, radiology must transition toward low-carbon and climate-resilient systems, with innovations that reduce emissions and environmental impact while preserving the quality of care. PCD-CT exemplifies this shift by delivering high-quality images at lower radiation doses and reduced contrast volume. It is particularly valuable in screening and long-term surveillance, where cumulative exposure is a concern. Future directions include broader clinical validation, integration with AI-based workflows, and incorporation into guidelines that reflect diagnostic excellence and environmental stewardship, while taking into account both the advantages of PCD-CT and its challenges, such as high cost and substantial power consumption.

In conclusion, PCD-CT represents not only a technological innovation but also a meaningful step toward more responsible and forward-looking radiologic practice. Its continued development will help ensure that thoracic oncology imaging remains both clinically effective and environmentally conscious.

### Footnotes

#### Conflict of interest disclosure

The authors declared no conflicts of interest.

### References

1. Pourmorteza A, Symons R, Sandfort V, et al. Abdominal imaging with contrast-enhanced photon-counting CT: first human experience. *Radiology*. 2016;279(1):239-245. [\[Crossref\]](#)
2. Willeminck MJ, Persson M, Pourmorteza A, Pelc NJ, Fleischmann D. Photon-counting CT: technical principles and clinical prospects. *Radiology*. 2018;289(2):293-312. [\[Crossref\]](#)
3. Nakamura Y, Higaki T, Kondo S, Kawashita I, Takahashi I, Awai K. An introduction to photon-counting detector CT (PCD CT) for radiologists. *Jpn J Radiol*. 2023;41(3):266-282. [\[Crossref\]](#)
4. Higaki F, Hiramatsu M, Yasuhara T, et al. Cranial and spinal computed tomography (CT) angiography with photon-counting detector CT: comparison with angiographic and operative findings. *Jpn J Radiol*. 2025;43(2):143-151. [\[Crossref\]](#)
5. Flohr T, Schmidt B. Technical basics and clinical benefits of photon-counting CT. *Invest Radiol*. 2023;58(7):441-450. [\[Crossref\]](#)
6. Fletcher JG, Inoue A, Bratt A, et al. Photon-counting CT in thoracic imaging: early clinical evidence and incorporation into clinical practice. *Radiology*. 2024;310(3):e231986. [\[Crossref\]](#)

7. Si-Mohamed S, Boccalini S, Rodesch PA, et al. Feasibility of lung imaging with a large field-of-view spectral photon-counting CT system. *Diagn Interv Imaging*. 2021;102(5):305-312. [\[Crossref\]](#)
8. Symons R, Cork TE, Sahbaee P, et al. Low-dose lung cancer screening with photon-counting CT: a feasibility study. *Phys Med Biol*. 2017;62(1):202-213. [\[Crossref\]](#)
9. Bartlett D, Koo CW, Bartholmai BJ, et al. High-resolution chest computed tomography imaging of the lungs: impact of 1024 matrix reconstruction and photon-counting detector computed tomography. *Invest Radiol*. 2019;54(3):129-137. [\[Crossref\]](#)
10. Schiebler ML, Jinzaki M, Yanagawa M, et al. Future applications of cardiothoracic CT. *Radiology*. 2025;315(3):e240085. [\[Crossref\]](#)
11. Hata A, Yanagawa M, Ninomiya K, et al. Photon-counting detector CT radiological-histological correlation in cadaveric human lung nodules and airways. *Invest Radiol*. 2025;60(2):151-160. [\[Crossref\]](#)
12. Inoue A, Johnson TF, Walkoff LA, et al. Lung cancer screening using clinical photon-counting detector computed tomography and energy-integrating-detector computed tomography: a prospective patient study. *J Comput Assist Tomogr*. 2023;47(2):229-235. [\[Crossref\]](#)
13. Prayer F, Kienast P, Strassl A, et al. Detection of post-COVID-19 lung abnormalities: photon-counting CT versus same-day energy-integrating detector CT. *Radiology*. 2023;307(1):e222087. [\[Crossref\]](#)
14. Inoue A, Johnson TF, White D, et al. Estimating the clinical impact of photon-counting-detector CT in diagnosing usual interstitial pneumonia. *Invest Radiol*. 2022;57(11):734-741. [\[Crossref\]](#)
15. Yanagawa M, Han J, Wada N, et al. Advances in concept and imaging of interstitial lung disease. *Radiology*. 2025;315(2):e241252. [\[Crossref\]](#)
16. Pannenbecker P, Huflage H, Granz JP, et al. Photon-counting CT for diagnosis of acute pulmonary embolism: potential for contrast medium and radiation dose reduction. *Eur Radiol*. 2023;33(11):7830-7839. [\[Crossref\]](#)
17. Hattori A, Suzuki K, Matsunaga T, et al. Is limited resection appropriate for radiologically "solid" tumors in small lung cancers? *Ann Thorac Surg*. 2012;94(1):212-215. [\[Crossref\]](#)
18. Hattori A, Matsunaga T, Takamochi K, Oh S, Suzuki K. Importance of ground glass opacity component in clinical stage IA radiologic invasive lung cancer. *Ann Thorac Surg*. 2017;104(1):313-320. [\[Crossref\]](#)
19. Koike H, Ashizawa K, Tsutsui S, et al. Surgically resected lung adenocarcinoma: do heterogeneous GGNs and part-solid nodules on thin-section CT show different prognosis? *Jpn J Radiol*. 2023;41(2):164-171. [\[Crossref\]](#)
20. Sasaki T, Kuno H, Nomura K, et al. CZT-based photon-counting-detector CT with deep-learning reconstruction: image quality and diagnostic confidence for lung tumor assessment. *Jpn J Radiol*. 2025;43(7):1132-1144. [\[Crossref\]](#)
21. Wang J, Huang Z, Zhu Z, et al. Photon-counting detector CT provides superior subsolid nodule characterization compared to same-day energy-integrating detector CT. *Eur Radiol*. 2025;35(6):2979-2989. [\[Crossref\]](#)
22. Prakash P, Kalra MK, Ackman JB, et al. Diffuse lung disease: CT of the chest with adaptive statistical iterative reconstruction technique. *Radiology*. 2010;256(1):261-269. [\[Crossref\]](#)
23. Funama Y, Taguchi K, Utsunomiya D, et al. Combination of a low-tube-voltage technique with hybrid iterative reconstruction (iDose) algorithm at coronary computed tomographic angiography. *J Comput Assist Tomogr*. 2011;35(4):480-485. [\[Crossref\]](#)
24. Gervaise A, Osemont B, Lecocq S, et al. CT image quality improvement using adaptive iterative dose reduction with wide-volume acquisition on 320-detector CT. *Eur Radiol*. 2012;22(2):295-301. [\[Crossref\]](#)
25. Katsura M, Matsuda I, Akahane M, et al. Model-based iterative reconstruction technique for ultralow-dose chest CT: comparison of pulmonary nodule detectability with the adaptive statistical iterative reconstruction technique. *Invest Radiol*. 2013;48(4):206-212. [\[Crossref\]](#)
26. Yanagawa M, Gyobu T, Leung AN, et al. Ultra-low-dose CT of the lung: effect of iterative reconstruction techniques on image quality. *Acad Radiol*. 2014;21(6):695-703. [\[Crossref\]](#)
27. Araki S, Kitagawa K, Kokawa T, et al. Radiation exposure in cardiac computed tomography imaging in Mie prefecture in 2021. *Jpn J Radiol*. 2023;41(6):596-604. [\[Crossref\]](#)
28. Hamabuchi N, Ohno Y, Kimata H, et al. Effectiveness of deep learning reconstruction on standard to ultra-low-dose high-definition chest CT images. *Jpn J Radiol*. 2023;41(12):1373-1388. [\[Crossref\]](#)
29. Hosokawa T, Kawakami H, Tanabe Y, et al. Left atrial strain assessment using cardiac computed tomography in patients with hypertrophic cardiomyopathy. *Jpn J Radiol*. 2023;41(8):843-853. [\[Crossref\]](#)
30. Murota M, Norikane T, Yamamoto Y, et al. An analysis of the left top pulmonary vein and comparison with the right top pulmonary vein for lung resection by three-dimensional CT angiography and thin-section images. *Jpn J Radiol*. 2023;41(9):965-972. [\[Crossref\]](#)
31. Fukamatsu F, Yamada A, Yamada K, et al. Serial assessment of computed tomography angiography for pulmonary and systemic arteries using a reduced contrast agent dose for the diagnosis of systemic artery-to-pulmonary artery shunts. *Jpn J Radiol*. 2024;42(5):460-467. [\[Crossref\]](#)
32. Kobayashi T, Kunihiro Y, Uehara T, Tanabe M, Ito K. Volume changes of diseased and normal areas in progressive fibrosing interstitial lung disease on inspiratory and expiratory computed tomography. *Jpn J Radiol*. 2024;42(8):832-840. [\[Crossref\]](#)
33. Ohno Y, Aoki T, Endo M, et al. Machine learning-based computer-aided simple triage (CAST) for COVID-19 pneumonia as compared with triage by board-certified chest radiologists. *Jpn J Radiol*. 2024;42(3):276-290. [\[Crossref\]](#)
34. Frings M, Welsner M, Mousa C, et al. Low-dose high-resolution chest CT in adults with cystic fibrosis: intraindividual comparison between photon-counting and energy-integrating detector CT. *Eur Radiol Exp*. 2024;8(1):105. [\[Crossref\]](#)
35. Graafen D, Emrich T, Halfmann MC, et al. Dose reduction and image quality in photon-counting detector high-resolution computed tomography of the chest: routine clinical data. *J Thorac Imaging*. 2022;37(5):315-322. [\[Crossref\]](#)
36. Horst KK, Hull NC, Thacker PG, et al. Pilot study to determine whether reduced-dose photon-counting detector chest computed tomography can reliably display Brody II score imaging findings for children with cystic fibrosis at radiation doses that approximate radiographs. *Pediatr Radiol*. 2023;53(6):1049-1056. [\[Crossref\]](#)
37. Bayfield KJ, Weinheimer O, Boyton C, et al. Implementation and evaluation of ultra-low dose CT in early cystic fibrosis lung disease. *Eur Respir J*. 2023;62(1):2300286. [\[Crossref\]](#)
38. Bosch de Basea M, Thierry-Chef I, Harbron R, et al. Risk of hematological malignancies from CT radiation exposure in children, adolescents and young adults. *Nat Med*. 2023;29(12):3111-3119. [\[Crossref\]](#)
39. Johnson JN, Hornik CP, Li JS, et al. Cumulative radiation exposure and cancer risk estimation in children with heart disease. *Circulation*. 2014;130(2):161-167. [\[Crossref\]](#)
40. National Lung Screening Trial Research Team; Aberle DR, Adams AM, et al. Reduced lung-cancer mortality with low-dose computed tomographic screening. *N Engl J Med*. 2011;365(5):395-409. [\[Crossref\]](#)
41. Zensen S, Bos D, Opitz M, et al. Radiation exposure and establishment of diagnostic reference levels of whole-body low-dose CT for the assessment of multiple myeloma with second- and third-generation dual-source CT. *Acta Radiol*. 2022;63(4):527-535. [\[Crossref\]](#)
42. El Bakkali J, Doudouh A. Comparison between InterDosi and MCNP in the estimation of photon SAFs on a series of ICRP pediatric voxelized phantoms. *Jpn J Radiol*. 2023;41(12):1420-1430. [\[Crossref\]](#)
43. Hagen F, Walder L, Fritz J, et al. Image quality and radiation dose of contrast-enhanced chest-CT acquired on a clinical photon-counting detector CT vs. second-

- generation dual-source CT in an oncologic cohort: preliminary results. *Tomography*. 2022;8(3):1466-1476. [\[Crossref\]](#)
44. Sawall S, Klein L, Amato C, et al. Iodine contrast-to-noise ratio improvement at unit dose and contrast media volume reduction in whole-body photon-counting CT. *Eur J Radiol*. 2020;126:108909. [\[Crossref\]](#)
  45. Zhang M, Nie K, Yuan D, et al. Reduction of radiation dose and contrast medium volume in photon-counting detector computed tomography head and neck angiography: a comparison to energy-integrating detector computed tomography. *Acta Radiol*. 2025;S1076-6332(25)00660-9. [\[Crossref\]](#)
  46. Emrich T, O'Doherty J, Schoepf UJ, et al. Reduced iodinated contrast media administration in coronary CT angiography on a clinical photon-counting detector CT system: a phantom study using a dynamic circulation model. *Invest Radiol*. 2023;58(2):148-155. [\[Crossref\]](#)
  47. Nakaura T, Ito R, Ueda D, et al. The impact of large language models on radiology: a guide for radiologists on the latest innovations in AI. *Jpn J Radiol*. 2024;42(7):685-696. [\[Crossref\]](#)
  48. Jiang B, Li N, Shi X, et al. Deep learning reconstruction shows better lung nodule detection for ultra-low-dose chest CT. *Radiology*. 2022;303(1):202-212. [\[Crossref\]](#)
  49. Kawata N, Iwao Y, Matsuura Y, et al. Prediction of oxygen supplementation by a deep-learning model integrating clinical parameters and chest CT images in COVID-19. *Jpn J Radiol*. 2023;41(12):1359-1372. [\[Crossref\]](#)
  50. Svalkvist A, Fagman E, Vikgren J, et al. Evaluation of deep-learning image reconstruction for chest CT examinations at two different dose levels. *J Appl Clin Med Phys*. 2023;24(3):e13871. [\[Crossref\]](#)
  51. Tang R, Li J, Zhao P, et al. Utility of machine learning for identifying stapes fixation on ultra-high-resolution CT. *Jpn J Radiol*. 2024;42(1):69-77. [\[Crossref\]](#)
  52. Nagayama Y, Emoto T, Kato Y, et al. Improving image quality with super-resolution deep-learning-based reconstruction in coronary CT angiography. *Eur Radiol*. 2023;33(12):8488-8500. [\[Crossref\]](#)
  53. Nakamoto A, Onishi H, Ota T, et al. Contrast-enhanced thin-slice abdominal CT with super-resolution deep learning reconstruction technique: evaluation of image quality and visibility of anatomical structures. *Jpn J Radiol*. 2025;43(3):445-454. [\[Crossref\]](#)
  54. Yanagawa M, Tsubamoto M, Satoh Y, et al. Lung adenocarcinoma at CT with 0.25-mm section thickness and a 2048 matrix: high-spatial-resolution imaging for predicting invasiveness. *Radiology*. 2020;297(2):462-471. [\[Crossref\]](#)
  55. Ninomiya K, Yanagawa M, Tsubamoto M, et al. Prediction of solid and micropapillary components in lung invasive adenocarcinoma: radiomics analysis from high-spatial-resolution CT data with 1024 matrix. *Jpn J Radiol*. 2024;42(6):590-598. [\[Crossref\]](#)
  56. Kim D, Ahn C, Kim JH. Impact of deep learning 3D CT super-resolution on AI-based pulmonary nodule characterization. *Tomography*. 2025;11(2):13. [\[Crossref\]](#)
  57. Xing X, Li L, Sun M, et al. Deep-learning-based 3D super-resolution CT radiomics model: predict the possibility of the micropapillary/solid component of lung adenocarcinoma. *Heliyon*. 2024;10(13):e34163. [\[Crossref\]](#)
  58. Wang S, Liu X, Jiang C, et al. CT-based super-resolution deep learning models with attention mechanisms for predicting spread through air spaces of solid or part-solid lung adenocarcinoma. *Acad Radiol*. 2024;31(6):2601-2609. [\[Crossref\]](#)
  59. Flohr TG, McCollough CH, Bruder H, et al. First performance evaluation of a dual-source CT (DSCT) system. *Eur Radiol*. 2006;16(2):256-268. Erratum in: *Eur Radiol*. 2006;16(6):1405. [\[Crossref\]](#)
  60. Karçaaltıncaba M, Aktaş A. Dual-energy CT revisited with multidetector CT: review of principles and clinical applications. *Diagn Interv Radiol*. 2011;17(3):181-194. [\[Crossref\]](#)
  61. Deng L, Yang J, Jing M, et al. Differentiating invasive thymic epithelial tumors from mediastinal lung cancer using spectral CT parameters. *Jpn J Radiol*. 2023;41(9):973-982. [\[Crossref\]](#)
  62. Takumi K, Nagano H, Myogasako T, et al. Feasibility of iodine concentration and extracellular volume fraction measurement derived from the equilibrium phase dual-energy CT for differentiating thymic epithelial tumors. *Jpn J Radiol*. 2023;41(1):45-53. [\[Crossref\]](#)
  63. Huang HC, Huang YS, Chang YC, et al. Dual energy computed tomography for evaluating nodal staging in lung adenocarcinoma: correlation with surgical pathology. *Jpn J Radiol*. 2024;42(6):468-475. [\[Crossref\]](#)
  64. Centen JR, Greuter MJW, Prokop M. Detectability of iodine in mediastinal lesions on photon counting CT: a phantom study. *Diagnostics (Basel)*. 2025;15(6):696. [\[Crossref\]](#)
  65. Urbaski S, Bache S, Rajagopal J, Samei E. Quantitative performance of photon-counting CT at low dose: virtual monochromatic imaging and iodine quantification. *Med Phys*. 2023;50(9):5421-5433. [\[Crossref\]](#)
  66. Si-Mohamed S, Bar-Ness D, Sigovan M, et al. Multicolour imaging with spectral photon-counting CT: a phantom study. *Eur Radiol Exp*. 2018;2(1):34. [\[Crossref\]](#)
  67. Kravchenko D, Gnasso C, Schoepf UJ, et al. Gadolinium-based coronary CT angiography on a clinical photon-counting-detector system: a dynamic circulating phantom study. *Eur Radiol Exp*. 2024;8(1):118. [\[Crossref\]](#)
  68. Rockall AG, Allen B, Brown MJ, et al. Sustainability in radiology: position paper and call to action from ACR, AOSR, ASR, CAR, CIR, ESR, ESRNM, ISR, IS3R, RANZCR, and RSNA. *Radiology*. 2025;314(3):e250325. [\[Crossref\]](#)